FLOW CALCULATIONS IN PELTON TURBINES. PART 2: FREE SURFACE FLOWS.

CALCULS D'ÉCOULEMENT DANS LES TURBINES PELTON. 2ÈME PARTIE: ÉCOULEMENTS À SURFACE LIBRE.

F. AVELLAN, PH. DUPONT, S. KVICINSKY, *Swiss Federal Institute of Technology, Hydraulic Machines Laboratory, Avenue de Cour 33, CH-1007 Lausanne, Switzerland*

L. CHAPUIS, E. PARKINSON, G. VULLIOUD, *Hydro Vevey S.A. Rue des Deux Gares 6, CH-1800 Vevey, Switzerland*

ABSTRACT

Hydraulic machine design can now take advantage of advanced flow calculation methods which are made available by several CFD software companies. Thanks to these recent developments, the so called "Volume Of Fluid" (VOF) methods can be now used for the analysis of the free surface flows in a Pelton Turbine. The aim of this paper is to evaluate this VOF approach with respect to the computation of the jet at the outlet of a Pelton injector and its trajectory in the buckets.

RÉSUMÉ

La conception des machines hydrauliques bénéficie actuellement de méthodes avancées de calculs d'écoulement qui sont mises à disposition par plusieurs sociétés de logiciels de calculs d'écoulements. Grâce à ces développements récents, la méthode de Volume de Fluide (VOF) peut être utilisée aujourd'hui pour l'analyse des écoulements à surface libre que l'on retrouve dans les turbines. Le but de cet article est d'évaluer cette méthode VOF pour le calcul du jet en sortie d'un injecteur de turbine Pelton et de sa trajectoire dans les augets.

1. INTRODUCTION

Free surface flows are characteristic of impulse turbines and lead to a specific numerical treatment for their studies. It is maybe the reason why the forming jet at the injector outlet and the impact on the bucket were rarely modeled (see [1], [2]); furthermore, as far as we know, no comparison with experimental data are available in the open literature.

The aim of the present study is to propose a reliable method to predict the flow in Pelton injectors and buckets. The benefit of such a calculation is to better determine the flow in such components, and, for example, to be able to evaluate the effects of the jet quality on the runner performances, regarding the efficiency as well as the risk of erosion due to cavitation as put to the fore by some authors ([3], [7] and [8]). In the same way, the knowledge of the pressure field acting in the bucket will allow an optimization of the shape of this latter using advanced fracture and fatigue calculation programs.

This article presents a validation study of a method called "Volume-Of-Fluid" (VOF) which is promising for the calculations of free surface flows in different cases related to hydraulic machinery. This method consists in a filling process of a meshed domain initially empty. The meshed domain corresponds to the volume susceptible to be filled by the flow. The calculation is done in two steps: first a Navier-Stokes calculation is performed on the filled part of the mesh, and then the convection of the fluid through the mesh is determined based on the calculated velocity field. This method is also used to predict unsteady cavitation with some interesting results ([5] and [6]).

After a general presentation of the VOF method, an application example is given in the first part of the article which shows how to calculate a planar jet impinging an oblique wall. This simple calculation allows to check the physical consistency of the results of the VOF method and helps to understand how the free surface location is calculated.

In the second part of the article, the results of the computation of the jet formed by the injector of a Pelton turbine and the water layer formed in a runner bucket are presented. These results are compared to experimental data for both cases. In the case of the Pelton bucket, the calculation is done in a stationary frame of reference. Possibilities to perform these calculations in the case of a rotating frame of reference are discussed with respect to the experimental results obtained in both cases.

2. GENERAL DESCRIPTION OF THE VOLUME-OF-FLUID METHOD

The Volume-Of-Fluid method (VOF) represents a powerful tool in simulating complex free surface deformations including folding and breakup. Free surfaces are characterized by a volume-of-fluid type representation on a fixed mesh. Advection of the fluid is followed by a volume tracking method. On the basis of a given velocity field, the volume tracking method determines a new fluid boundary. On the basis of a given fluid boundary, the Reynolds Average Navier-Stokes equations are solved using the finite element method to predict kinematics. These two methods are thus applied in an alternating and non coupled fashion in order to calculate free surface deformations. A full description of the method and its implementation in the commercial CFD software used for that study is available in [4].

The fluid volume is represented by F, a characteristic marker concentration function.

The value of F is unity within the tracked fluid and zero outside. Steep gradients in the marker concentration represent free surface locations. The advection of the marker concentration F is governed by

$$\frac{\partial F}{\partial t} + \vec{u} \cdot \nabla F = 0 . \qquad (1)$$

Sharp interfaces are maintained by ensuring sharp gradients in F. This is achieved by a special treatment of the advection term in the transport equation (1). Two different scenarii are possible with the commercial CFD software used for that study. In the first one, two immiscible fluids A and B exist within the computational domain and forces may appear between them. The full elements represent fluid A while the empty one represent fluid B. In the second scenario, a single fluid displaces a region of void. Full elements represent the fluid, and empty elements represent the void. This latter scenario is very interesting when dealing with water filling a volume initially occupied by air. As far as the forces at the interface of the two fluids are negligible, only the part filled with water is of interest. Then only filled elements are contributing to the system assembly, which is of highest interest concerning the memory usage as well as the computational time.

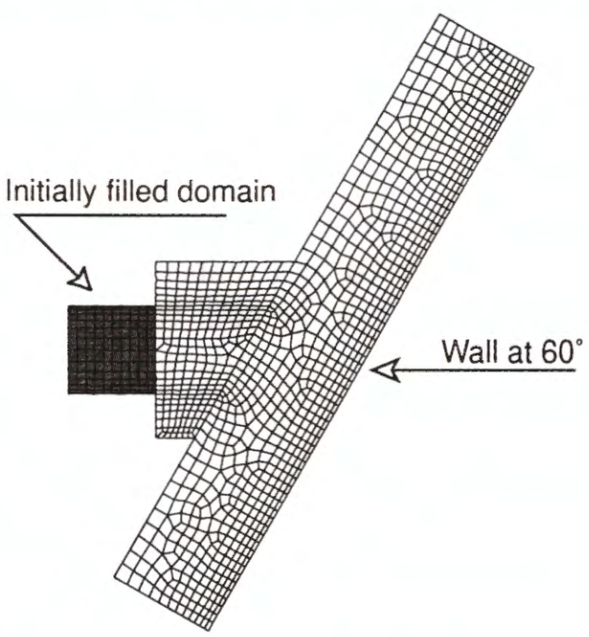

Figure 1: Mesh domain for the planar jet

The filling process is inherently transient. This implies to perform the calculation with a transient approach, which could be time consuming. For the problem concerning the prediction of the flow in the Pelton buckets, this limitation is not relevant. The flow is essentially unsteady, the jet being in a stationary frame of reference, while the bucket is in a rotating frame of reference. The calculation of the water sheet spreading in a bucket presented at the end of this article is nevertheless done in a stationary frame of reference, and compared to measurements done in a similar situation. This is due to the fact that some present limitations concerning the boundary conditions linked with the filling process need to be improved in order to allow the filling conditions to vary in time.

In order to introduce the way the free surface is treated with the VOF approach, we present here a simple example corresponding to the propagation of a two-dimensional planar jet against an inclined wall. The Figure 1 gives the mesh used for that calculation. As explained, the propagation of the jet is a time-dependant phenomenon which needs to be solved as unsteady. Initially, only a part of the mesh

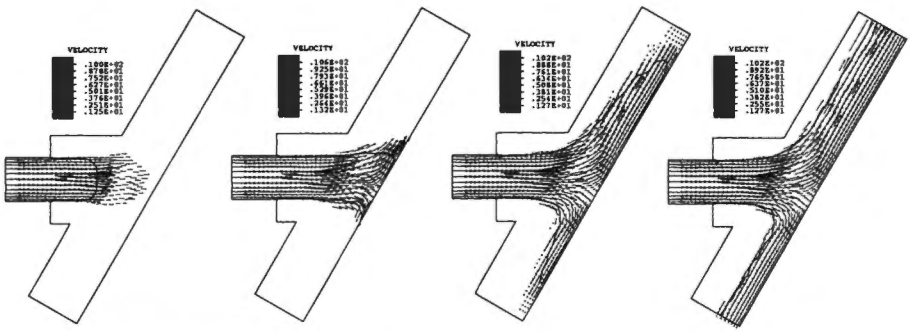

Figure 2: Jet flow convection in the meshed domain.

is filled, corresponding for example to the pipe from which the jet is issued. The rest of the mesh is empty, but the mesh domain corresponds to the most probable geometric part to be filled (see Figure 1).

Different time steps of the filling process are given on Figure 2, the last one corresponding to the steady state reaches at the end of the calculation. The black curve displayed on all the drawings on Figure 2 figures the interface location corresponding to a value of the marker concentration F equal to 0.5. As one can notice on this figure, some elements outside this limit are partially filled. This is due to the fact that the interface is defined within one or two adjacent elements, which leads, if the mesh is too coarse, to a poor definition of the interface location.

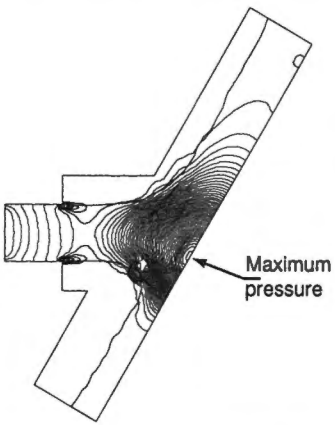

Figure 3: Pressure contours in the jet.

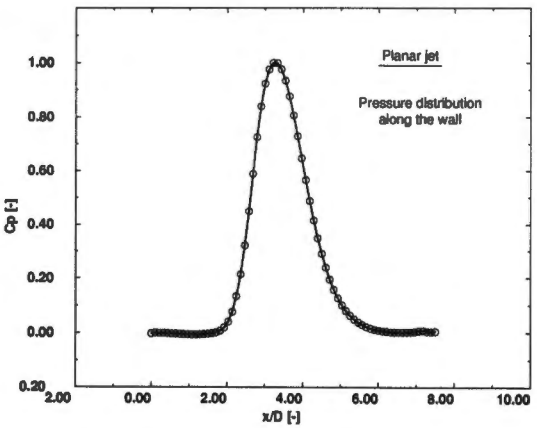

Figure 4: Pressure distribution along the wall.

It can be observed on Figure 3 that the maximum pressure point, corresponding to the stagnation point, is not aligned with the axis of the impinging jet. This well known result obtained with inclined walls is well reproduced by the calculation.

Figure 4 shows the pressure coefficient distribution along the inclined wall for the last time step corresponding to the steady state. This maximum pressure coefficient corresponds, as expected, to the stagnation pressure, and the minimum pressure to zero, at both ends of the planar jet. This example shows the ability of the VOF method to capture phenomenon similar to that observed in a Pelton runner.

3. FLOW IN AN AXISYMMETRIC INJECTOR

Calculations have been performed for the geometry of an axisymmetric injector. The geometry of this injector is given on Figure 5 and a close view of the corresponding mesh around the outlet of the injector is given on Figure 6.

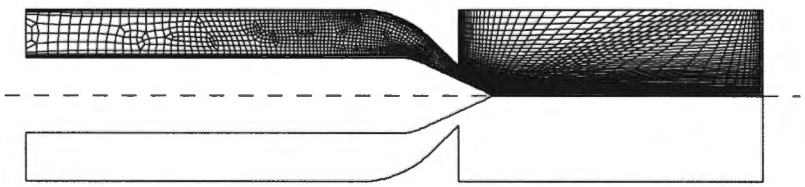

Figure 5: Geometry of the axisymmetric injector

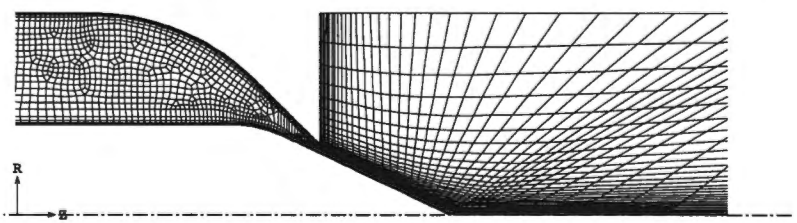

Figure 6: Close view of the mesh at the injector outlet

The flow is considered to be axisymmetric, unsteady, viscous and turbulent, but without swirl components. The calculations have been performed for different positions of the needle. These positions correspond to needle strokes C_p relative to the outlet radius of the injector R_d of respectively C_p/R_d = 0.3, 0.6, 1.0 and 1.8. The inlet conditions correspond to a head of 100 meters and a turbulence level of 2 percents. Measurements of the contracted radius of the jet at the outlet of the injector have been performed in similar conditions. These measurements are compared to the numerical results on Figure 7. The minimum jet radius R_{jet}, relative to the outlet diameter R_d is followed versus the relative needle stroke. The actual position of the interface corresponds to a value of the concentration marker *F* equal to 0.5. The error bars correspond to the thickness of the transition layer between the two extreme values of the function F.

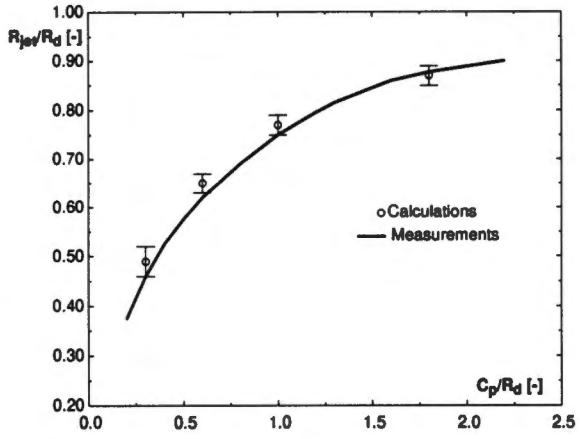

Figure 7: Comparison between measured and calculated jet radius.

It could be noticed that the calculation results agree quite well with the measurements. Moreover, no information is known about the precision of the measurements, but one can expect it to be of the same range then the calculation.

On Figure 8 are given velocity vectors fields at two different relative needle strokes, C_p/R_d = 0.3 and 0.6, and the corresponding absolute velocity for radial sections at three axial positions along the jet path, respectively x/R_d = 1, 2 and 3. The wake of the needle is well visible on the velocity vectors plotted for the two calculated strokes, associated to the low velocities corresponding to the darker color. The velocity profiles of Figure 8 show this wake to have completely disappeared at a distance of three radii from the outlet of the injector, for the two calculated conditions. This result is quite different from the one obtained in [2] where the velocity default in the wake of the needle is still very high

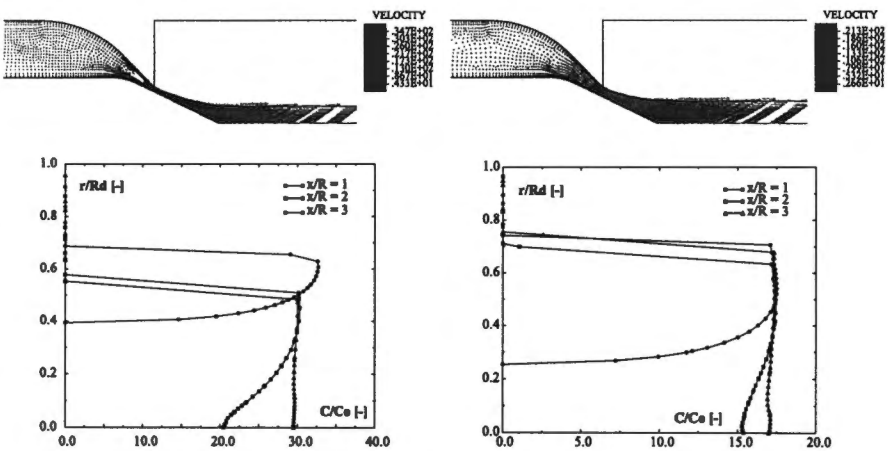

Figure 8: Velocity field (up) and absolute velocity profiles for three axial positions along the jet path (x/Rd = 1, 2 and 3) (down) at two relative needle strokes Cp/Rd = 0.3 and 0.6.

at four radii form the nozzle exit. This difference is probably due to the fact that the calculations presented here are made using a turbulence model, while the referenced calculation was a laminar one. The diffusion effect of the turbulence model is strong and very sensitive to the turbulence level given at the inlet flow. Unfortunately, without having any available experimental data for the velocity profiles across the jet, it is difficult to conclude.

4. FLOW IN A BUCKET

The last calculation done in this study is the quasi-steady computation of the water layer flow propagating in a bucket of a Pelton turbine. Present limitations of the code used in that study concerning the boundary conditions for the filling process prevent us to perform these calculations for a rotating bucket, i.e. for an angle between the jet and the bucket changing with respect to time. For that reason, the calculations have been performed for a stationary bucket, i.e. for a constant angle between the jet and the bucket. In order to validate these calculations, pressure measurements and visualizations have also been done on a model of a Pelton turbine in a test bed with a fixed runner. These pressure measurements have been compared to those measurements done with a rotating runner. In both cases, the needle stroke is kept constant, which corresponds to a nearly constant jet diameter. The tested conditions in the stationary configuration have been chosen to let the velocities correspond to the relative velocities in the rotating configuration at nominal head and for a given position of the bucket relative to the jet axis.

4.1 MEASUREMENTS

4.1.1 Pressure measurement

A bucket of a model runner has been equipped with miniature dynamic pressure transducers at two different locations A and B, see Figure 9. The experimental set-up used for measurements in both stationary and rotating conditions is the same. It consists of a conditioning electronic installed in a sealed box attached to the runner and using a voltage to frequency conversion to transmit the measured signals from the rotating part to the stationary part of the machine through slip rings. This experimental set-up is described in details in [9] and [10].

The conditions imposed for the measurements in the stationary configuration is a head of 18.57 meters, and an needle stroke of 17.1 mm, corresponding to a mean jet velocity of 19.09 $m \cdot s^{-1}$. This leads to a velocity equal to the relative velocity of the

Head [m]	P^*_A [bar]	P^*_B [bar]	Cp_A [-]	Cp_B [-]
18.57	0.27	0.24	0.149	0.132

Table 1: Pressure measured in the stationary configuration

jet in the rotating conditions with a nominal head of 75 meters and for an angle between the jet and the bucket splitter of 78°. The pressures p*, relative to the atmospheric pressure, and the pressure coefficients Cp at points A and B obtained for this configuration are summarized on Table 1. The pressure coefficient is given by p*/ρgH.

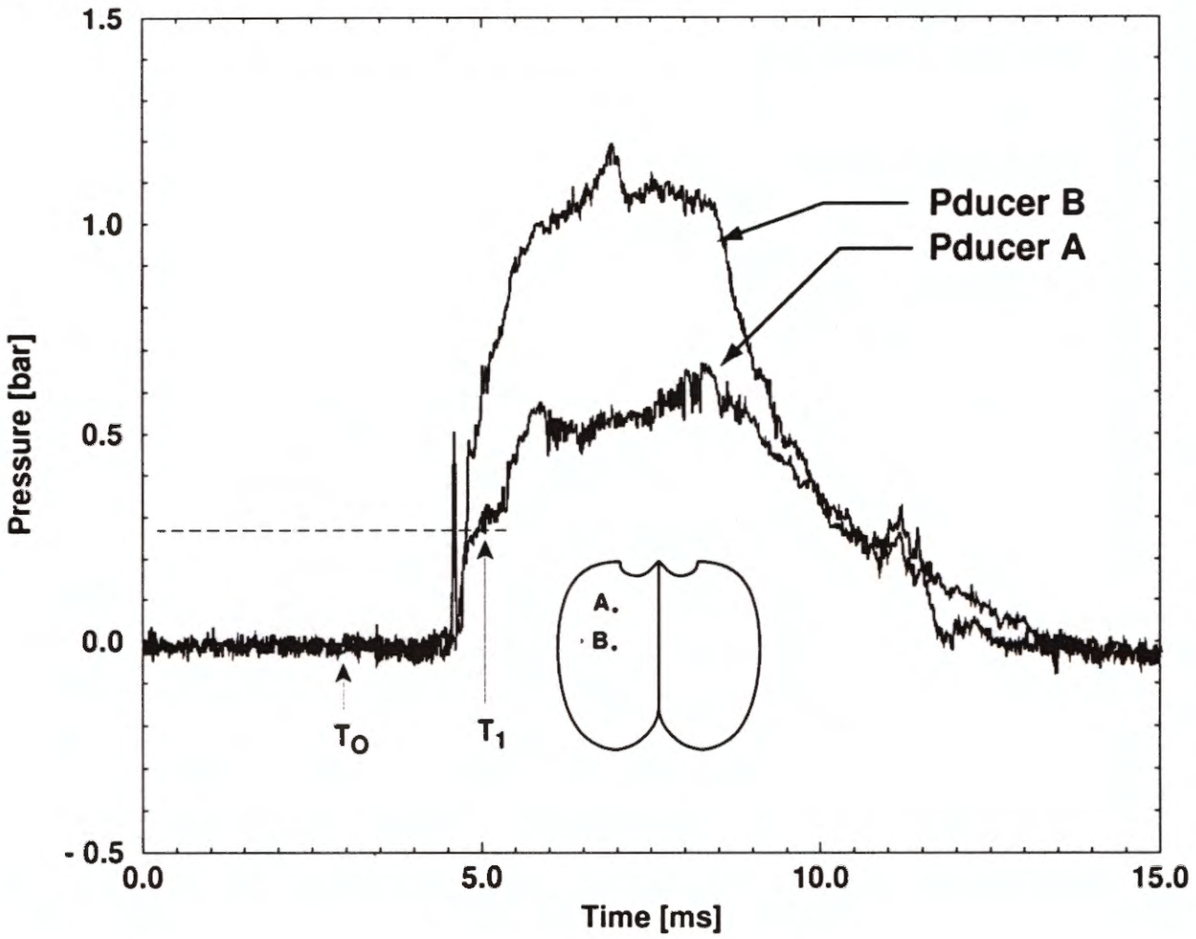

Figure 9: Unsteady pressure measurement in the rotating configuration with the pressure taps location.

The unsteady pressures obtained in the rotating configuration at nominal condition, i.e. a head of 75 m and a injector opening of 17.1 mm, are given on Figure 9 for the two measurements location A and B. This figure also shows the time T_0 corresponding to the first contact between the jet and the bucket splitter, and the time T_1 corresponding to the position of the bucket relative to the jet axis equal to 78°, which is the position used for the stationary configuration. One can observe that the pressure values at time T1 for pressure tap A agree well with the one measured in the stationary bucket. As stated in [3], the flow appearances in a stationary system are practically the same as in a rotating system. It is then possible to make investigation of flow in a stationary bucket which would contribute deeply to the knowledge of the flow.

4.1.2 Visualization

Side views and face views are obtained through tubes to prevent the splashing water flowing along the casing side walls to screen the windows. These visualizations give good information about the flow pattern and the flow angles. On the face view on Figure 10, one can observe the part of the flow escaping from the cutout of the bucket as well as the lateral sheet flow. On the side view on Figure 11, the direction of the flow getting out from the bucket is easily observed. On the same picture, the fan-shaped flow coming out of the cutout is also visible.

The ability of the VOF method to provide similar pattern than visualization allows us to use this method to overcome future operation problem as it is praticed during model test [11].

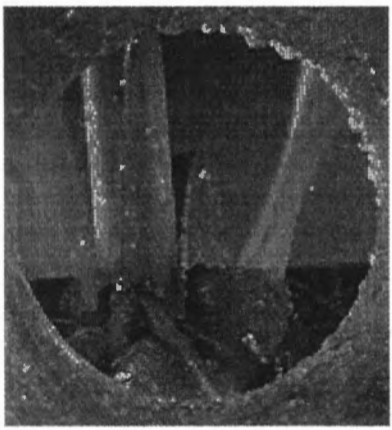

Figure 10: Face view of the jet in the stationary bucket

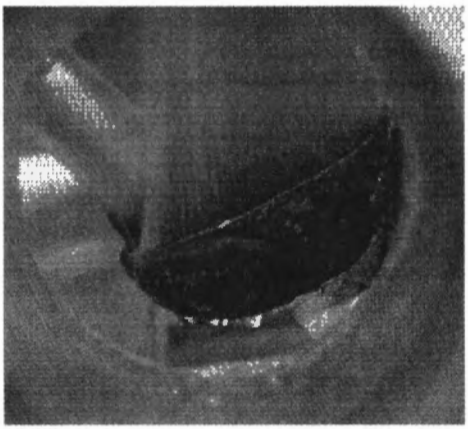

Figure 11: Side view of the jet in the stationary bucket

4.2 CALCULATION RESULTS

The calculation of the water layer in the bucket has been performed on the half on the bucket, using a symmetric condition in the center plane of the two spoons forming the bucket. The meshing of the volume inside the bucket and over it has been done using 80,000 unstructured hexahedric elements. At initial time, only a part of the cylinder corresponding to the jet path is filled. On this initially filled part, a velocity equal to the relative velocity is imposed. Then the convection of this fluid is calculated using the VOF approach. A mixing-length turbulence model is used for the calculation.

On Figure 12 and Figure 13, shaded water layer and velocity vectors are displayed using the same points of view as the one used for the visualizations on Figure 10 and Figure 11. One can observe that the flow pattern calculated is very closed to the one visualized on the stationary bucket. The part of the flow going out from the cutout as

well as the outlet flow angles are very similar. On Figure 14, the upper view of the calculated velocities shows the path of the flow in the bucket. The thickness of the liquid sheet is shown to be non uniform along the outlet edge of the bucket. Indeed, for that particular jet incidence angle, the water sheet is thicker at mid span of the bucket and thinner closer to the root of the bucket. Consequently, the velocities are higher close to the root than at mid span of the bucket. The information on the water layer thickness and on the outlet flow allow to optimize the wall angles at the outlet edge of the bucket in order to avoid any interference with the neighbouring bucket.

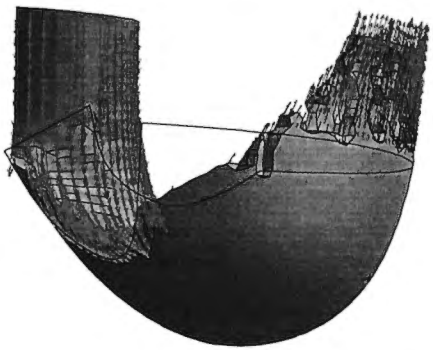

Figure 12: Face view of the calculated flow in the bucket

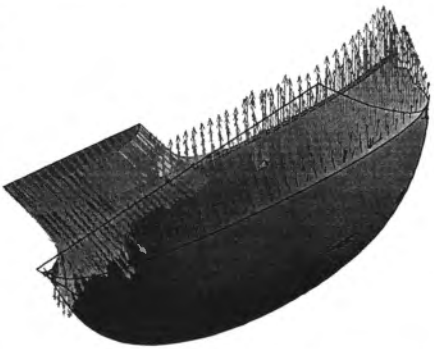

Figure 13: Side view of the calculated flow in the bucket

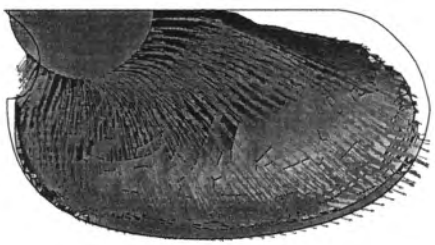

Figure 14: Upper view of the calculated flow in the bucket

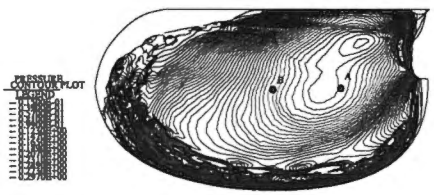

Figure 15: Bottom view of the pressure field acting on the bucket

Figure 15 gives the pressure field on the bucket wall. It can be first observed that the calculated pressures are close to the measured one, but not equal. At the location corresponding to pressure taps A and B, the calculated pressures are respectively , 0.26 and 0.22. It has to be said that this result is obtained for a time corresponding to the flow reaching the outlet edge of the bucket. The pressures for that specific case are probably not exactly equal to the one obtained at the steady condition. In that sense, one can notice the overpressure zones, in red, close to the outlet edge. This overpressure has been observed to be linked with the front of the jet attached to the

wall. Due to viscous forces, the jet is propagating slower close to the wall, resulting in a local over pressure. This has been measured in a former experimental test ([8]) in rotating conditions, but not during the present one.

5. DISCUSSION AND CONCLUSION

The ability of a Volume-of-Fluid approach to calculate free surface flows in Pelton turbine has been shown. Results obtained for the jet coming out from an injector and the sheet flow propagating in a stationary bucket of a Pelton turbine have been successfully compared to experimental data. Presently, only the flow in a stationary bucket has been addressed due to limitation of the boundary conditions available for the filling process. This limitation should be overcome soon and a calculation of the flow in a bucket in a rotating frame of reference with a impinging jet direction changing with time will be then possible. Nevertheless, the total computational time on a SGI Origin 2000 using 8 processors to follow the entire propagation of the jet in the stationary bucket is about 40 hours with the CFD code used. This is obviously not a usable tool for development at present, but one can expect the machines and the algorithms in the near future to be fast enough to reduce this time by a factor of ten. This approach will then be a very useful tool to optimize bucket design.
The results obtained and presented in this article show the potential of the VOF method for the calculation of free surface flows, in particular for Pelton turbines. Hopefully in the near future, this method can be used to optimize the geometry of these machines and to have a better understanding of the mechanical loading of the bucket.

6. ACKNOWLEDGMENT

The study was possible through the financial support of the Swiss Federal "Commission pour l'Innovation et la Technologie" (CTI). The authors would like to thank Mr. Ritter for his help in performing the first calculations, to Mr. J.-F. Caron for his help in performing the pressure measurements in the Pelton turbine bucket, and to the staff of the Hydro Vevey laboratory for having made possible the model tests.

7. REFERENCES

[1] Nonoshita, T., Matsumoto, Y., Kubota, T., Ohashi, H., Calculation of the Jet Accompanied with Water Droplets in a Pelton Turbine, ASME 95, FED-Vol. 226, Cavitation and Gas-Liquid Flow in Fluid Machinery, pp. 111+117, Hilton Head Island, USA, 1995

[2] Nonoshita, T., Matsumoto, Y., Kubota, T., Ohashi, H., Numerical Simulation of Jet in a Pelton Turbine, Proceedings of the XVIII IAHR Symposium on

Hydraulic Machinery and Cavitation, Vol. 1, pp. 352÷360, Valencia, Spain, 1996

[3] Lowy, R., Efficiency Analysis of Pelton Wheels, Transactions of the A.S.M.E., August, 1944.

[4] FIDAP 7.5 Update Manual, January 1995, Revision 7.5, 1st Edition

[5] Diéval, L., Marcer, R., Arnaud, M., Modélisation de poches de cavitation par une méthode de suivi d'interface de type VOF, Journal de la Houille Blanche, N° 4/5, pp. 96÷99, 1997

[6] Diéval, L., Arnaud, M., Rouault, M.C., Numerical Modelling Emergence of a Cavitating Profile by a VOF Method, Moving Boundaries 97, 27-29 août 1997, Ghent, Belgique

[7] Brivio, R., Zappi, O., La cavitazione nelle turbine Pelton, (Parte I), L'ENERGIA ELECTTRICA, Vol. 72, N° 2, pp. 45-49, Mars-avril 1995

[8] Brivio, R., Zappi, O., La cavitazione nelle turbine Pelton, (Parte II), L'ENERGIA ELECTTRICA, Vol. 73, N° 4, pp. 266-270, Juillet-août 1996

[9] Bourdon, P., Farhat, M., Simoneau, R., Pereira, F., Dupont, Ph., Avellan, F., Dorey, J.-M., Cavitation Erosion Prediction on Francis Turbines. Part 1: Measurements on the Prototype, Proceedings of the XVIII IAHR Symposium on Hydraulic Machinery and Cavitation, Vol. 1, pp. 534÷543, Valencia, Spain, 1996

[10] Dupont, Ph., Caron, J.-F., Avellan, F., Bourdon, P., Lavigne, P., Farhat, M., Simoneau, R., Dorey, J.-M., Archer, A., Laperrousaz, E., Couston, M., Cavitation Erosion Prediction on Francis Turbines. Part 2: Model Tests and Flow Analysis, Proceedings of the XVIII IAHR Symposium on Hydraulic Machinery and Cavitation, Vol. 1, pp. 574÷583, Valencia, Spain, 1996

[11] Bachmann, P., Schärer, Ch., Staubli, T., Vullioud, G., Experimental Flow Studies on a 1-Jet Model Pelton Turbine, Proceedings of the 15th IAHR Symposium on Hydraulic Machinery and Cavitation, Vol. 2, R3, Belgrade, Yugoslavia, 1990